Solvation Effect on Kinetic Rate Constant of Reactions in Supercritical Solvents

A. A. Chialvo and P. T. Cummings
Dept. of Chemical Engineering, University of Tennessee, Knoxville, TN 37996
Chemical Technology Div., Oak Ridge National Laboratory, Oak Ridge, TN 37831

Yu. V. Kalyuzhnyi
Institute for Condensed Matter Physics, Svientsitskoho 1, 290011 Lviv, Ukraine

A statistical mechanical analysis of the solvation effects on the kinetic rate constants of reactions in near and supercritical solvents is presented to understand the experimental findings regarding the thermodynamic pressure effects. This is an extension of the solvation formalism of Chialvo and Cummings to the analysis of the microscopic basis for the macroscopic pressure and temperature effects on the kinetic rate constants of reactions conducted in the compressible region of the solvent phase diagram. This analysis is illustrated with integral equations calculations involving Lennard–Jones infinitely dilute quaternary systems to describe the species in solution during the reaction of triplet benzophenone (^3BP) with a cosolvent (either O_2 or 1,4-cyclohexadiene) in supercritical CO_2 along the supercritical isotherms $T_r = 1.01$ and 1.06. The role of the species molecular asymmetries and consequently their solvation behavior in determining the thermodynamic pressure and temperature effects on the kinetic rate constant of reactions at near-critical conditions are discussed.

Introduction

Chemical reactions at supercritical conditions have recently become the focus of intense fundamental research because of their potential application to environmentally friendly new technologies such as waste treatment, material processing, biomass to fuel conversion, as well as electrochemical and enzymatic reactions (Hutchenson and Foster, 1995; Kiran and Brennecke, 1993; Kiran and Levelt Sengers, 1994; Levelt Sengers, 1991a). While the most compelling reason to carry out reactions at (near) supercritical conditions is our ability to tune the solvation conditions of the medium (chemical potentials) and attentuate transport limitations by adjustment of the system pressure and/or temperature (Bruno and Ely, 1991; McHugh and Krukonis, 1994), there has been considerable speculation on explanations for the *unusual* behavior (occasionally referred to as *anomalies*) in reaction kinetics at near and supercritical conditions (for a summary see (Brennecke, 1993; Clifford, 1994; Savage et al., 1995)). Strictly speaking, one expects that true near-critical anomalies in reaction equilibria, if any, will manifest themselves only within an extremely small neighborhood of the system's critical point (Milner and Martin, 1986; Wheeler and Petschek, 1983), which is unattainable for all practical purposes. This is because the near-critical anomaly in the equilibrium extent of reaction has the same near-critical behavior as the internal energy, that is, $\sim [(T - T_c)/T_c]^{1-\alpha}$ with $\alpha \cong 0.12$. However, it is not as clear that the kinetics of reactions should be free of anomalies in the near-critical region. Therefore, a more accurate description of *solvent effect* on the kinetic rate constant of reactions conducted in or near supercritical media is desirable and is the goal of our study.

The solvent effect (or, more precisely, the solvation effect) on the kinetic reaction rate has most frequently been interpreted within the framework of the transition state theory (TST) (Hynes, 1985; Reichardt, 1979; Steinfeld et al., 1989), and its thermodynamic formulation has become the most commonly used approach to study the changes of Gibbs free energy of activation, as well as its temperature and pressure derivatives, because it gives a simple mathematical form for inter- and extrapolation purposes. Solvation plays a significant role in reacting systems not only by affecting the kinetic rate but also the reaction selectivity, resulting from the differential stabilization (or preferential solvation) of reactants, products, and transition state (TS) species according to the strength of their molecular asymmetries with respect to the solvent (Hynes, 1985; Reichardt, 1979; Steinfeld et al., 1989).

The thermodynamic approach to solvation effects on reaction rates was earlier pursued to study atom-transfer reactions (Benson, 1960; Moelwyn-Hughes, 1971), by invoking a wide variety of new concepts for its implementation, such as free volume (Benson, 1960; Frost and Pearson, 1961), solubilities (Bell, 1939; Martin, 1966), and TS boiling points (Benson and Golden, 1975). More recently, it has been suggested that the experimental isothermal kinetic rate constants of some reactions at near and supercritical conditions could not be explained solely by the thermodynamic pressure effect, but from the combination of local composition enhancement and density augmentation around reactants (Brennecke, 1993; Bunker and Sun, 1995; Chateauneuf et al., 1992; Ellington and Brennecke, 1993; Savage et al., 1995).

Although these variations on the TST argument have often been successful in providing qualitative agreement with experimentally observed trends, they have not yielded quantitative predictions of the solvation effect on the reaction rate. One possible reason for this lack of quantitative prediction is that the main players in the approach, the species solvation properties, are *microscopic* quantities that, in macroscopic modeling, are indirectly described by *macroscopic* properties, which are difficult to measure or hard to predict accurately.

In this article we attempt to rationalize the experimental findings and their interpretations by drawing an explicit link between the thermodynamic pressure or temperature effect (macroscopic) and the species solvation (microscopic) behavior through a statistical mechanical analysis of the reaction rate constant at near and supercritical conditions. Because this solvation approach (Chialvo and Cummings, 1994, 1995) hinges upon the rigorous Kirkwood–Buff's fluctuation formalism of mixtures (Kirkwood and Buff, 1951), and it is applied to precisely defined model mixtures, we are able to make unambiguous connections between the species molecular asymmetries, the solution microstructure, and the kinetically relevant macroscopic properties.

Furthermore, throughout this work we use integral equations (IE) calculations for Lennard–Jones infinitely dilute quaternary systems to study a simple model for the pressure dependence of the kinetic rate constant for the reaction of triplet benzophenone (^{3}BP) with a solvent (either O_2, or 1,4-cyclohexadiene) in supercritical CO_2 (Roberts et al., 1995a,b). The IE calculations are used not only to generate the microstructural details of the systems, but also to calculate the required macroscopic thermophysical properties involved in the determination of the pressure effect on the kinetic rate constant. In doing so, we maintain an internal consistency between the microstructure and the corresponding (macroscopic) thermophysical properties.

The article is organized as follows. First we introduce the main expressions behind the application of the formalism to the kinetic problem, whose details are given in the Appendix. Then, we illustrate the approach with integral equations calculations, and discuss the results in terms of molecular asymmetries and solvation behavior of species in solution. Finally, we discuss briefly some aspects of the use and validity of the TST for reaction kinetics at near-critical conditions.

Fundamentals

In this section we present the main ideas behind the solvation approach to studying the thermodynamic pressure effect on the kinetic reaction rate constant. We must emphasize that we are considering solely *equilibrium solvent effects* on the kinetic rate constant according to the TST formalism: that is, while the possibility of the breakdown of the TST hypotheses caused by the solvent dynamics is another important issue to consider, it will not be addressed here (Hynes, 1985).

With that purpose let us assume the following simple reaction,

$$\nu_R R + \nu_S S \xrightleftharpoons{\text{solvent}} \mathfrak{R}^{\ddagger} \rightarrow \textit{products} \tag{1}$$

where R is a solute reactant, S is the cosolvent, $\mathfrak{R}^{\ddagger}$ is the activated complex in equilibrium with the reactants in solution, and the prefactors are the stoichiometry coefficients. Here we consider the case in which the cosolvent might participate in the reaction as reactants.

According to the TST of reactions (Hynes, 1985; Steinfeld et al., 1989), the reaction rate constant is given by

$$k^{TST} = \frac{kTK_0}{\hbar} K_c^{\ddagger}, \tag{2}$$

where k and $\hbar$ are the Boltzmann and Planck constants, respectively, T is the absolute temperature, K_0 is a factor that gives the correct units for k^{TST}, and $K_c^{\ddagger}$ is the molar-based equilibrium constant for the activation process given by Eq. 1. In order to study the pressure effect on the kinetic rate constant, we first rewrite $K_c^{\ddagger}$ in terms of the species fugacities, and then determine the pressure coefficient of $\ln k^{TST}$ (see Appendix A for details),

$$\left(\frac{\partial \ln k^{TST}}{\partial P}\right)_{T,x} = -\Delta\nu\kappa + (\nu_R \bar{v}_R^{\infty} + \nu_S \bar{v}_S^{\infty} - \nu_{\mathfrak{R}} \bar{v}_{\mathfrak{R}}^{\infty})/kT \tag{3}$$

where $\Delta\nu^{\ddagger} = \nu_R \bar{v}_R^{\infty} + \nu_S \bar{v}_S^{\infty} - \nu_{\mathfrak{R}} \bar{v}_{\mathfrak{R}}^{\infty}$ is the actual activation volume (Eckert, 1972).

Typically the actual kinetic rate constant k_{exptl} is obtained from k^{TST} by correcting the latter by the transmission coefficient χ, which takes care of the actual barrier recrossing, that is, $k_{\text{exptl}} = \chi k^{TST}$. Moreover, it is frequently assumed that $\chi \neq \chi(P,T)$ or taken as unity (the TST case). This is a very important assumption that should be borne in mind (Hynes, 1985; Steinfeld et al., 1989), and that will be discussed later.

Although Eq. 3 gives a macroscopic expression for the pressure derivative of the TST kinetic rate constant, it will allow us to introduce the solvation contributions in a precisely microscopic way. To achieve this goal we express the partial molar volumes in terms of the derivative $(\partial P/\partial x_u)_{T,\rho,x_{k \neq u}}^{\infty}$, whose critical value is the corresponding Krichevskii's parameter (Levelt Sengers, 1991a) for the infinitely dilute solute species labeled by the subscript u. This derivative is an appealing quantity because it measures the isothermal–isochoric finite pressure change induced by the solvent rearrangement in the solvation of an infinitely dilute solute (Chialvo and Cummings, 1994, 1995; Chialvo et al., 1996), and allows us to make an explicit separation between solvation and compressibility-driven contributions to the species partial molar volumes at infinite dilution. In fact, and according to Appendix A, Eq. 3 can be rewritten either as

$$\left(\frac{\partial \ln k^{TST}}{\partial P}\right)_{T,x} = \Delta\nu(\kappa^{IG} - \kappa) - \kappa\rho[\nu_{\Re}(\bar{v}_{\Re}^{\infty}(SR) - \rho^{-1}) - \nu_R(\bar{v}_R^{\infty}(SR) - \rho^{-1}) - \nu_S(\bar{v}_S^{\infty}(SR) - \rho^{-1})] \quad (4)$$

or

$$\left(\frac{\partial \ln k^{TST}}{\partial P}\right)_{T,x} = \kappa\rho[\nu_R(\bar{v}_R^{\infty}(SR) - \bar{v}_R^{\infty(IG)}(SR) + \nu_S(\bar{v}_S^{\infty}(SR) - \bar{v}_S^{\infty(IG)}(SR)) - \nu_{\Re}(\bar{v}_{\Re}^{\infty}(SR) - \bar{v}_{\Re}^{\infty(IG)}(SR))], \quad (5)$$

where $\rho = (1/\bar{v}_\nu^0)$, the superscripts *IG* denote ideal gas properties, and the solvation contribution to the partial molar volumes $\bar{v}_u^{\infty}(SR)$ can be interpreted microscopically in terms of either total or direct correlation function integrals, as discussed in detail in (Chialvo and Cummings, 1994, 1995; Chialvo et al., 1996) and summarized in Appendix A. Thus, the pressure coefficient of the rate constant can be factorized into two terms: one involving the solvent's isothermal compressibility, and the other containing short-range solvation contributions to the species in solutions relative to their ideal gas contributions (absence of solute–solvent interactions). Note that the difference $(\bar{v}_u^{\infty}(SR) - \bar{v}_u^{\infty(IG)}(SR))$ actually subtracts the translational or "ideal gas" contribution from the $\bar{v}_u^{\infty}(SR)$, and therefore, contains only contributions from intermolecular interactions. Moreover, for reactions with $\Delta\nu = 0$, the "ideal gas" contributions cancel out, see Eqs. 4–5, and the pressure effect becomes equal to the solvation contribution to the activation volume, $[\nu_R\bar{v}_R^{\infty}(SR) + \nu_S\bar{v}_S^{\infty}(SR) - \nu_{\Re}\bar{v}_{\Re}^{\infty}(SR)]$, magnified by the solvent's isothermal compressibility.

According to Eqs. 4–5, whatever the isothermal thermodynamic pressure effect might be, this becomes predominant at near-critical conditions unless the coefficient of the isothermal compressibility, the solvation factor, is zero (a truly unlikely situation). Our previous statistical mechanical analysis indicated that $\rho\bar{v}_u^{\infty}(SR)$ is a well-behaved finite quantity (Chialvo and Cummings, 1994, 1995), a conclusion that can also be reached through purely thermodynamic arguments (Levelt Sengers, 1991a). Since thermodynamic stability demands that the solvent isothermal compressibility be positive, the solvation factor determines the sign of the pressure effect at near-critical conditions. This prefactor is a function of the relative molecular asymmetry between the solute reactant and the activated complex (as well as the solvent, should this participate in the reaction).

The advantage of this formalism resides in that it does not rely on any assumption regarding type of interactions or molecular asymmetry, number of components in solution, or pairwise additivity, and only requires the center-of-mass spatial distribution functions of species in solution as descriptors of the system's microstructure (Kirkwood and Buff, 1951). Thus most thermophysical properties, including the ones involved in the solvation process, are determined as integrals over the microstructure of the system (i.e., the radial distribution functions for the solute–solute, solute–solvent, and solvent–solvent interactions). Yet, in order to take full advantage of this formalism we must be able to generate the system's microstructure from the knowledge of the species molecular asymmetries (force-field parameters of the intermolecular models). For this purpose here we use integral equation calculations for Lennard–Jones systems to generate the solution microstructures, and consequently, the solvation macroscopic properties to determine the pressure effects on the kinetic rate constant of a model reaction.

Integral Equations Calculations

In this section we illustrate the solvation behavior of Lennard–Jones mixtures composed of a solvent and three infinitely dilute species, one of them being a cosolvent. These model systems provide a very much simplified model of the actual reacting systems studied by Roberts et al. (1995a,b), that is, the triplet benzophenone (^{3}BP) as an infinitely dilute reactant, either O_2 or 1,4-cyclohexadiene as an infinitely dilute reactive cosolvent, the infinitely dilute transition state species (TS), and the supercritical solvent CO_2. Even though our goal is not to mimic the actual system, the reasons behind the choice of this model are manifold, namely: (1) we know the phase diagram for the pure solvent with adequate accuracy (Panagiotopoulos, 1987), that is, we can locate our system relative to the solvent critical point using corresponding state variables ($\rho_r = \rho/\rho_c$, $T_r = T/T_c$, where the subscript c denotes critical conditions); (2) the near-critical (divergent) effects are common to any (real or model) fluid system exhibiting liquid–vapor critical behavior, that is, there is no need for a realistic model to get useful insight into the near-critical solvation phenomenon; (3) the solution of the Ornstein Zernicke equation via the Percus–Yevick approximation gives an accurate representation of the Lennard–Jones fluid (Barker and Henderson, 1976); and (4) because we generate the entire solvation thermodynamics and structural information, using the same formalism for a (microscopically) well-defined system, we eliminate any possible ambiguity in the interpretation of the theoretical results.

Tables 1 and 2 show the force-field parameters for the species used in this study. Unlike interactions are initially described by the Lorentz (size) and Berthelot (energy) combining rules (Hansen and McDonald, 1986). In a subsequent step, we might perturb these combining rules, especially for the solvent–TS interactions to assess the extent to which our imperfect (due to the lack of better experimental information) description of the TS molecular asymmetry might change the outcome of the pressure dependence of the kinetic rate constant.

Table 1. Lennard–Jones Potential Parameters for the Reacting Quaternary Mixture

Interaction Type	Epsilon/*k* (K)	Sigma (Å)
CO_2–CO_2	232.2	3.643
O_2–O_2	119.0	3.355
^{3}BP–^{3}BP	625.7	6.580
TS–TS*	681.7	7.291

*Parameters determined from the critical properties given by Roberts et al. (1995a,b).

Table 2. Lennard–Jones Potential Parameters for the Reacting Quaternary Mixture

Interaction Type	Epsilon/k (K)	Sigma (Å)
CO_2–CO_2	232.2	3.643
1,4-C6–1,4-C6*	436.7	5.227
^3BP–^3BP	625.7	6.580
TS–TS**	791.8	8.247

*1,4-cyclohexadiene.
**Parameters determined from the critical properties given by Roberts et al. (1995a,b).

To interpret the possible preferential solvation of the ^3BP around the cosolvent, and to make contact with the measured rate constants, we also study the solvation effects on the pressure dependence of the kinetic rate constant when the repulsive cosolvent O_2 is replaced by the attractive cosolvent 1,4-cyclohexadiene. By repulsive and attractive (Debenedetti and Mohamed, 1989) cosolvents we mean that their associate $(\partial P/\partial x_u)^{\infty}_{T,\rho,x_{k\neq u}}$ will be positive and negative, respectively, that is, they will behave as volatile and nonvolatile species, respectively (Levelt Sengers, 1991a).

The study of the cosolvent effect on reactivity, and the concomitant solvation features, is intended to provide insight on the possible connection between the local cosolvent composition around the reactant ^3BP (preferential solvation) and the resulting pressure or temperature effect on the kinetic rate constant.

Partial molar volumes of species in solution

Because the partial molar volume of species in solution plays the most important role in this formalism, we first determine the density dependence for the three species at infinite dilution along the near-critical isotherms $T_r = 1.01$ and $T_r = 1.06$ as shown in Figures 1 and 2 in comparison with the corresponding $\bar{v}_u^{\infty}(SR)$. (Note that because 100 volume units ≈ 2.9 L/mol in these illustrations, the species partial molar volumes at near-critical conditions vary from 3 L/mol (oxygen) to -30 L/mol (transition state complex). In contrast, the corresponding solvation contributions go from 0.15 L/mol to -1.45 L/mol.)

For illustration purposes, we have also included in these pictures the properties of two limiting cases, a "solute" in the ideal solution (IS), that is, the pure solvent, and the ideal gas solute (IG). These cases are very convenient references because they encompass two extreme molecular asymmetries, that is, the presence of intermolecular forces with no solute–solvent asymmetry, and the absence of solute–solvent interactions, respectively. Moreover, the difference $\bar{v}_u^{\infty}(SR) - \bar{v}_u^{\infty}(IS) = \bar{v}_u^{\infty}(SR) - \rho^{-1}$ is the so-called *solute-induced effect*, the actual volumetric contribution to the solvation driving force (Chialvo and Cummings, 1994, 1995).

As the solute becomes less repulsive, with respect to that of an ideal gas (see Appendix A), $(\partial P/\partial x_u)^{\infty}_{T,\rho,x_{k\neq u}}$ reaches zero for the IS, and then becomes negative for the more pronounced molecular asymmetries (see Figures 3 and 4). Note that this function can show an extreme finite value at a density greater or smaller than the critical, depending on the molecular asymmetry, with the exception of the IS for which $(\partial P/\partial x_u)^{\infty}_{T,\rho,x_{k\neq u}} = 0$ at any state condition. Correspondingly, the partial molar volumes $\bar{v}_u^{\infty}$ becomes less positive as we turn on the molecular interactions (IG → IS), and reaches large negative values as we increase the molecular asymmetry

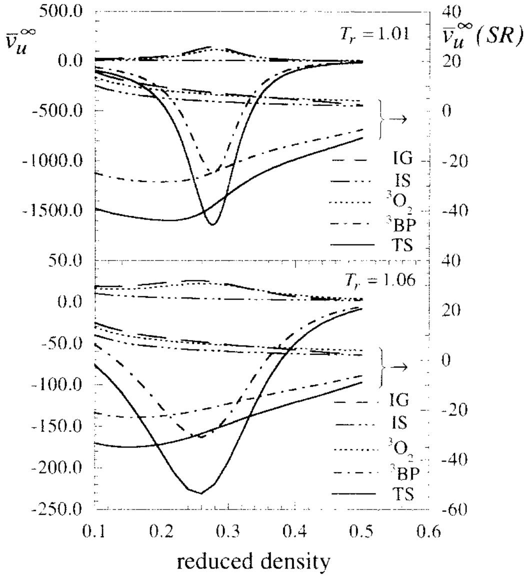

Figure 1. Density dependence of species partial molar volume $\bar{v}_u^{\infty}$ and its solvation counterpart $\bar{v}_u^{\infty}(SR)$ at $T_r = 1.01$ (upper) and $T_r = 1.06$ (lower) for the reactive system $^3BP + {}^3O_2 + CO_2 \Leftrightarrow TS$.

Density and volumes in units of $\sigma^3_{CO_2}$ and $(1/\sigma^3_{CO_2})$, respectively.

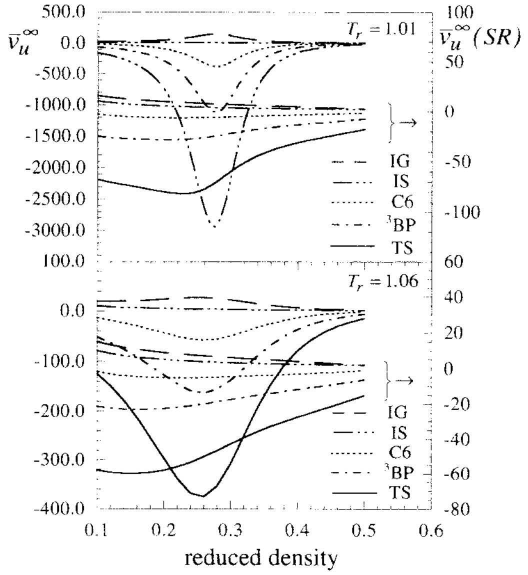

Figure 2. Density dependence of species partial molar volume $\bar{v}_u^{\infty}$ and its solvation counterpart $\bar{v}_u^{\infty}(SR)$ at $T_r = 1.01$ (upper) and $T_r = 1.06$ (lower) for the reactive system $^3BP + 1,4\text{-}C_6 + CO_2 \Leftrightarrow TS$.

Density and volumes in units of $\sigma^3_{CO_2}$ and $(1/\sigma^3_{CO_2})$, respectively.

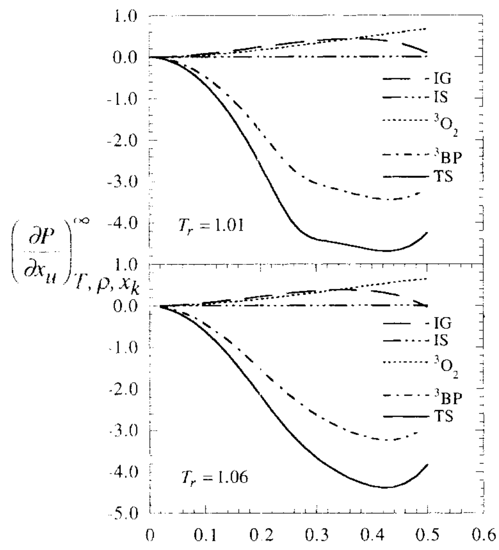

Figure 3. Density dependence of species $(\partial P/\partial x_u)^{\infty}_{\rho,T,x_{k\neq u}}$ at $T_r = 1.01$ (upper) and $T_r = 1.06$ (lower) for the reactive system $^3BP + {}^3O_2 + CO_2 \Leftrightarrow TS$.

Density and pressure in units of $\sigma^3_{CO_2}$ and $(\sigma^3_{CO_2}/\epsilon_{CO_2})$, respectively.

with respect to the solvent. In all cases, except for the IS, $\bar{v}_u^{\infty}$ exhibits an extreme value around the density where the isothermal compressibility does. In contrast, $\bar{v}_u^{\infty}(SR)$ shows positive values with a monotonic density change for the IG and IS cases. Then, for more pronounced asymmetries, $\bar{v}_u^{\infty}(SR)$ exhibits a positive extreme depending on the behavior of $(\partial P/\partial x_u)^{\infty}_{T,\rho,x_{k\neq u}}$.

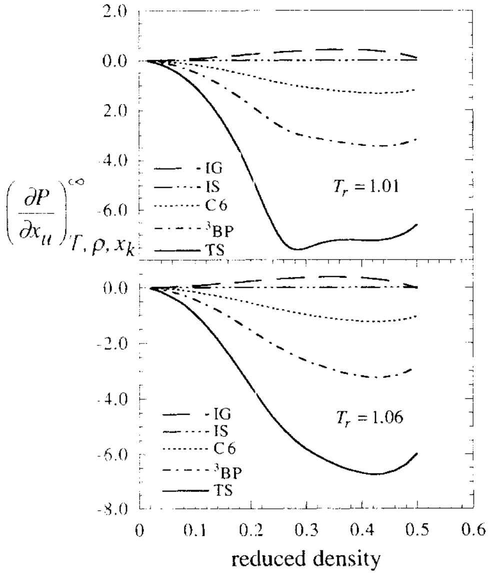

Figure 4. Density dependence of species $(\partial P/\partial x_u)^{\infty}_{\rho,T,x_{k\neq u}}$ at $T_r = 1.01$ (upper) and $T_r = 1.06$ (lower) for the reactive system $^3BP + 1,4\text{-}C_6 + CO_2 \Leftrightarrow TS$.

Density and pressure in units of $\sigma^3_{CO_2}$ and $(\sigma^3_{CO_2}/\epsilon_{CO_2})$, respectively.

The positive partial molar volume at infinite dilution exhibited by the oxygen, the signature of a volatile, $(\partial P/\partial x_u)^{\infty}_{T,\rho,x_{k\neq u}} > 0$ (Levelt Sengers, 1991b), or repulsive (Debenedetti and Mohamed, 1989) solute is the expected behavior for a dissolved gas in a near-critical solvent. In contrast, the 1,4-cyclohexadiene, the triplet benzophenone, and the corresponding transition state complexes (TS) exhibit the typical nonvolatile, $(\partial P/\partial x_u)^{\infty}_{T,\rho,x_{k\neq u}} < 0$, or attractive behavior usually associated with bulky (strongly interacting) solutes. This behavior can be clearly seen in Figures 3 and 4, where we display the corresponding density dependence for $(\partial P/\partial x_u)^{\infty}_{T,\rho,x_{k\neq u}}$, the macroscopic quantity that most succinctly characterizes the solvation phenomenon (Chialvo and Cummings, 1994, 1995; Chialvo et al. 1996).

Microstructural solvent behavior around reactants

The system's microstructure is characterized here by the spatial (radial) pair distribution functions for all possible like and unlike pair interactions (McDonald, 1973). In Figures 5 and 6 we display the radial distribution functions for the solvent–reactant and cosolvent–reactant interactions for the system $^3BP + {}^3O_2 + CO_2 \Leftrightarrow TS$ and $^3BP + 1,4\text{-}C_6 + CO_2 \Leftrightarrow TS$ at $T_r = 1.01$ and $\rho_r = 1.0$. All radial distribution functions decay to one (the local densities approach the bulk values) from above one, with the exception of that for the CO_2–O_2 interactions, which does it from below one. This behavior can be understood by considering that the introduction of a solute into the solvent induces a local perturbation of the solvent structure, whose magnitude depends on the strength of the solute–solvent interactions, and its effect propagates as far as the solvent correlation length allows. The magnitude of this (solvation) effect is macroscopically determined by $(\partial P/\partial x_u)^{\infty}_{T,\rho,x_{k\neq u}}$, and its (compressibility-driven) propagation is manifested by the slow-decaying tail of the radial distribution functions (Chialvo and Cummings, 1994, 1995).

When referring to the short-range microstructural features of a near or supercritical solvent around a dilute solute, the literature frequently highlights the fact that the solvent is lo-

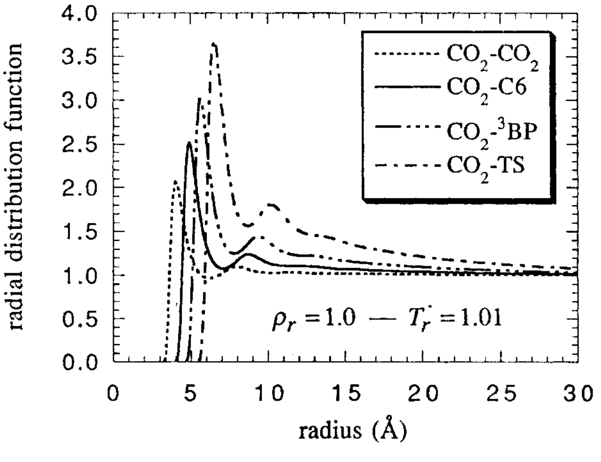

Figure 5. Solvent-solvent, solute-solvent, solute-cosolvent, transition state-solvent radial distribution functions for the reactive system $^3BP + 1,4\text{-}C_6 + CO_2 \Leftrightarrow TS$ at $T_r = 1.01$ and $\rho_r = 1.0$.

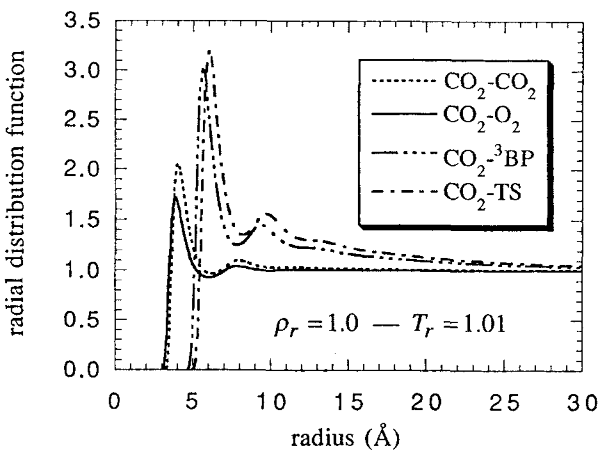

Figure 6. Solvent-solvent, solute-solvent, solute-cosolvent, transition state-solvent radial distribution functions for the reactive system ${}^3BP+{}^3O_2+CO_2 \Leftrightarrow TS$ at $T_r=1.01$ and $\rho_r=1.0$.

cally denser than its bulk value (Brennecke, 1993; Carlier and Randolph, 1993; Combes et al., 1992; Eckert and Knutson, 1993; Ellington et al., 1994; Savage et al., 1995; Sun and Bunker, 1995; Zhang et al., 1995). Likewise, when the near-critical system involves a cosolvent, the literature refers to the relative denser environments around species in solution in terms of local compositions differing from the global compositions (Brennecke, 1993; Chateauneuf et al., 1992; Ellington and Brennecke, 1993; Zhang et al., 1995).

It is worth noting, however, that this is not an inherently near-critical or supercritical mixture phenomenon: it occurs at all state conditions ranging from near-ideal gas mixtures to dense liquids. Levent Sengers (1991a,b) has argued, based on the series expansion of the residual Helmholtz free energy ($A^r(T,\rho_\nu^{-1},x_u)$) around the critical point of the pure solvent $x_u=0$, that the short-range solvent density augmentation or depletion around a solute should occur with similar results away from the critical point, and that the divergence of the solute partial molar volume is an incidental effect related only to the solvent's criticality. In fact, these thermodynamic arguments involve the coefficient $(\partial P/\partial x_u)^\infty_{T,\rho,x_{k\neq u}}$, which is a well-defined macroscopic analog of the microstructural changes induced by the solute–solvent molecular asymmetry in the solvation process (Chialvo and Cummings, 1994, 1995).

As previously suggested (Chialvo and Cummings, 1994), since a locally denser region of solvent is observed even around a solvent molecule at any state condition, the focus in solvation should be on the difference between solvent structure around a solute molecule and solvent structure around a solvent molecule. Moreover, with the exception of the IS, for which the strength of the like and unlike intermolecular interactions are all identically the same (and therefore the corresponding solute–solute, solute–solvent, and solvent–solvent pair distribution functions will be also identical to one another, indicating that neither species shows preference for any other), the relative molecular asymmetry in the intermolecular interactions will translate into microstructural arrangements (solvation shells) with enrichment (depletion) of one component over the other with respect to what we would find in the corresponding pure system (ideal solution). For example, in our model calculations at both near-critical conditions studied here ^{3}BP enriches its solvation shell over that of the corresponding pure solvent CO_2 (see Figure 5) and gives rise to solvent–solvent ($\nu\nu$) and solute–solvent total pair correlation integrals ($u\nu$) such that $G^0_{\nu\nu} < G^\infty_{u\nu}$, and according to Eq. A9, to $(\partial P/\partial x_u)^\infty_{T,\rho,x_{k\neq u}} < 0$ (see Figure 4), that is, an attractive or nonvolatile solute. Conversely, O_2 depletes its solvation shell over that of the corresponding pure solvent CO_2 (see Figure 6) and gives rise to $G^0_{\nu\nu} > G^\infty_{u\nu}$, with the consequent $(\partial P/\partial x_u)^\infty_{T,\rho,x_{k\neq u}} > 0$ (see Figure 3), that is, becoming a repulsive or volatile species.

These relative (to the ideal solution) changes in the solvation shell population (preferential solvation), measured by $(\partial P/\partial x_u)^\infty_{T,\rho,x_{k\neq u}}$, are the microstructural manifestation of the molecular asymmetry between solvent–solvent and solute–solvent interactions and take place *at any state conditions*, including the highly compressible regions of the solvent phase diagram. Indeed, preferential solvation has been theoretically studied and experimentally observed in aqueous organic and electrolyte systems under ambient conditions (Ben-Naim, 1988, 1990; Covington and Newman, 1976) for many years. In fact, there are two main aspects to consider, namely: (1) even a small degree of preferential solvation of one species over another (density perturbation) at near-critical conditions (in contrast to normal conditions) will be substantially magnified by compressibility effects (propagation of the perturbation), resulting in large partial molar volumes (see Eq. A6), and most importantly, (2) even if we (experimentally or theoretically) observed preferential solvation of the reactive solute and/or the dilute cosolvent, the pressure (temperature) coefficient of the kinetic rate constant does not depend on an individual species preferential solvation, or its partial molar volume counterpart, but on the relative solvation of all species in solution.

In particular, according to Eq. 5, the preferential solvation of a reactant by the dilute cosolvent has no direct impact on the pressure dependence of the kinetic rate constant. This is the message conveyed by the microscopic interpretation of the finite term in Eq. 5. In other words, for the specific reaction under study, we might observe preferential solvation of the reactive ^{3}BP in Figures 7 and 8, species *R*, by the solvent CO_2 over the dilute cosolvent O_2, species S, and conclude that the experimentally observed $(\partial \ln k_{\text{exptl}}/\partial P)_{T,x} > 0$ (see Figure 8 in Roberts et al., 1995b) is consistent with the idea of a local composition of cosolvent O_2 being lower than the solvent CO_2 around the reactive solute ^{3}BP. While this appears to be consistent with our IE calculations (Figure 9), the same argument would predict the local composition of 1,4-cyclohexadiene around the reactive solute ^{3}BP should be higher than the solvent CO_2, since the observed $(\partial \ln k_{\text{exptl}}/\partial P)_{T,x} < 0$ for the ${}^3BP+1{,}4\text{-}C_6+CO_2 \Leftrightarrow TS$ system. However, even though we observe preferential solvation of ^{3}BP by the 1,4-cyclohexadiene over CO_2, we also observe that $(\partial \ln k^{TST}/\partial P)_{T,x} > 0$ (Figure 10), that is, a similar behavior as for cosolvent O_2 and opposite to the experimentally determined quantity (see Figure 8 of Roberts et al., 1995b).

These results suggest that the connection between the cosolvent's preferential solvation of the reactants and the sign of the pressure effect within the TST framework can be more subtle than previously supposed, and propose that we must

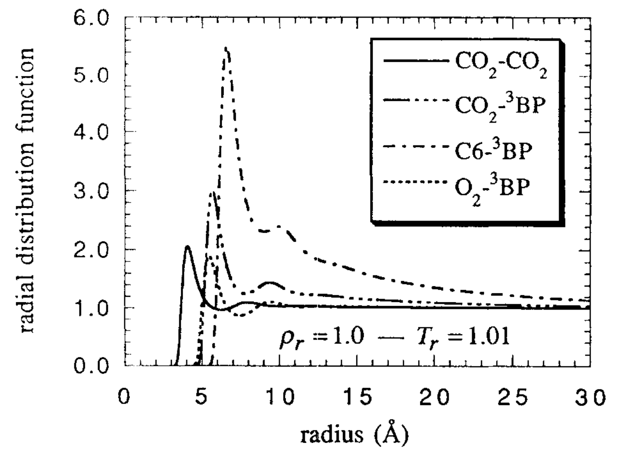

Figure 7. Radial distribution functions for the ^{3}BP–solvent (or cosolvent) interactions in comparison to that for the solvent–solvent at $T_r = 1.01$ and $\rho_r = 1.0$.

seek an explanation to this dilemma: What is wrong with the preferential solvation hypothesis in explaining the $(\partial \ln k^{TST}/\partial P)_{T,x}$ behavior? The answer lies in the missing solvation contribution of the TS (species $\Re^{\ddagger}$). According to Eq. 5 we cannot reach a meaningful conclusion about the connection between the solvation behavior and the pressure effects unless we analyze the (preferential) solvation of *all species* in solution, rather than that of an individual reactant alone. The obvious corollary to this statement is that we are also required to consider the molecular asymmetry of the TS with extreme caution, because of the large near-critical sensitivity of its partial molar properties to small perturbation of its molecular asymmetry (as analyzed below).

For the sake of illustration of this point, let us imagine the following molecular asymmetry between reactants and TS species: the TS and ^{3}BP have similar (but not necessarily identical) asymmetries with respect to the solvent CO$_2$ so that their solvation properties will also be similar to each other (actually both species exhibit similar molecular asymmetries in the $^3BP + {}^3O_2 + CO_2 \Leftrightarrow TS$, see Table 1 and Figures 1, 3, and 6). Moreover, for the sake of argument let us make the TS species equally or less attractive than ^{3}BP, meaning that $(\partial P/\partial x_{\Re})^{\infty}_{T,\rho,x_{k \neq \Re}} \geq (\partial P/\partial x_R)^{\infty}_{T,\rho,x_{k \neq R}}$. Then, even though ^{3}BP will be solvated preferentially by CO$_2$ rather than by O$_2$ (see Figure 8), the reaction will exhibit a $(\partial \ln k^{TST}/\partial P)_{T,x} < 0$ (Figure 9), rather than the positive experimentally observed value (Roberts et al., 1995b), because of the relative sizes of $(\partial P/\partial x_i)^{\infty}_{T,\rho,x_{k \neq i}}$ ($i = S$, R, $\Re^{\ddagger}$ in Eq. 5). Note that this behavior ($(\partial \ln k^{TST}/\partial P)_{T,x} < 0$) will show up even if $(\partial P/\partial x_{\Re})^{\infty}_{T,\rho,x_{k \neq \Re}} = (\partial P/\partial x_R)^{\infty}_{T,\rho,x_{k \leq R}} < 0$, that is, when the TS and the ^{3}BP are equally solvated.

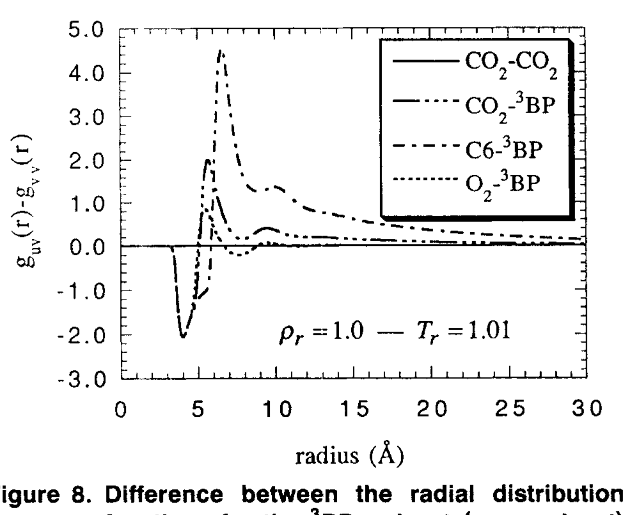

Figure 8. Difference between the radial distribution functions for the ^{3}BP–solvent (or cosolvent) interactions and that for the solvent–solvent interactions at $T_r = 1.01$ and $\rho_r = 1.0$.

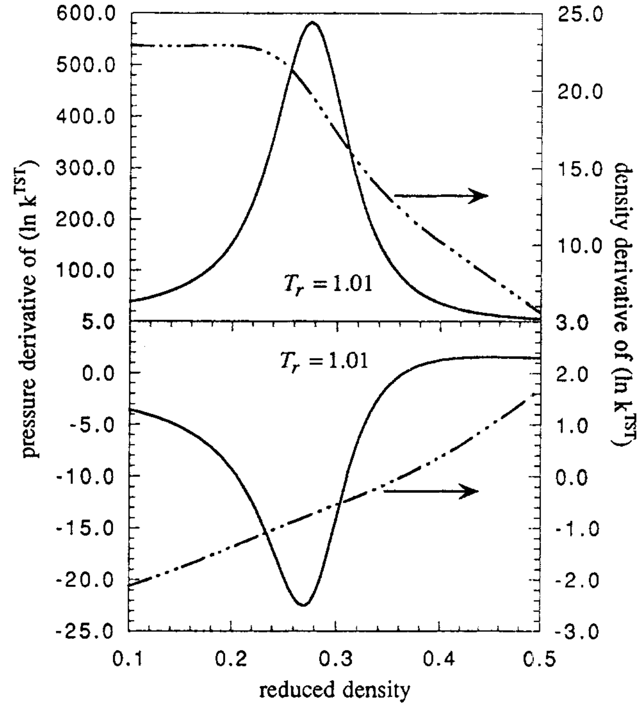

Figure 9. Comparison between $(\partial \ln k^{TST}/\partial P)_{T,x}$ and $(\partial \ln k^{TST}/\partial \rho)_{T,x}$ for the reactive system $^3BP + {}^3O_2 + CO_2 \Leftrightarrow TS$ and at $T_r = 1.01$ and $\rho_r = 1.0$, with ($\xi = (\epsilon_{uv}/\epsilon^B_{uv}) = 1.0$, $\eta = (\sigma_{uv}/\sigma^L_{uv}) = 1.0$) (upper), and ($\xi = (\epsilon_{uv}/\epsilon^B_{uv}) \approx 0.94$, $\eta = (\sigma_{uv}/\sigma^L_{uv}) \approx 0.93$) (lower).

Thus, the conclusion here is that we cannot suggest an explanation for the lack of agreement between the experimentally observed behavior of $(\partial \ln k_{\text{exptl}}/\partial P)_{T,x}$ and the corresponding behavior predicted by an equation of state (EOS), regardless of its lack of accuracy, unless we take into account the solvation behavior of *all* species in solution, *including* the TS complex. While the preferential solvation of the reactive solute might give, in some cases, a consistent interpretation of the experimentally observed behavior, it cannot by itself explain it because it does not give a complete account of *all* solvation effects. Moreover, caution must be exercised in the preceding calculations due to the lack of accuracy in the EOS predictions of solute partial molar volumes at near-critical conditions, as discussed by Eckert et al. (1983). A less obvious defect in these EOS calculations is associated with the

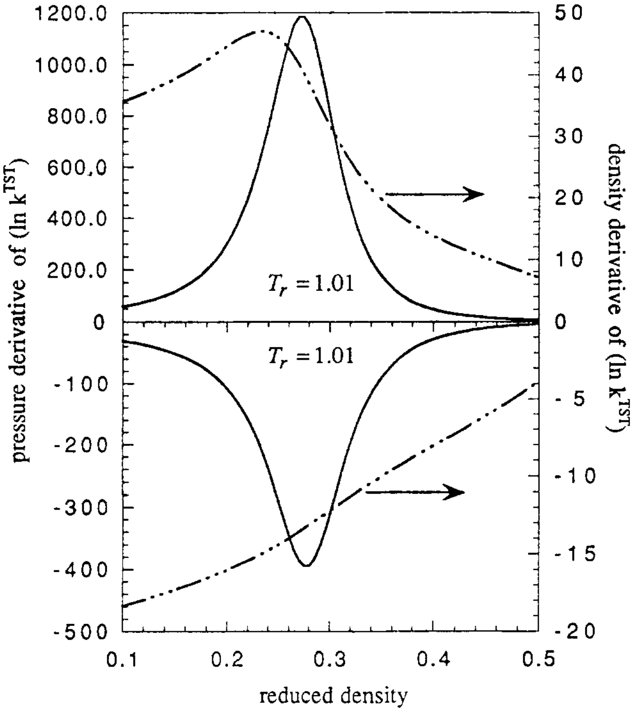

Figure 10. Comparison between $(\partial \ln k^{TST}/\partial P)_{T,x}$ and $(\partial \ln k^{TST}/\partial \rho)_{T,x}$ for the reactive system ^{3}BP +1,4-C$_6$ +CO$_2$ $\Leftrightarrow$ TS and at $T_r = 1.01$ and $\rho_r = 1.0$, with $(\xi = (\epsilon_{u\nu}/\epsilon_{u\nu}^B) = 1.0$, $\eta = (\sigma_{u\nu}/\sigma_{u\nu}^L) = 1.0)$ (upper), and $(\xi = (\epsilon_{u\nu}/\epsilon_{u\nu}^B) \approx 0.89$, $\eta = (\sigma_{u\nu}/\sigma_{u\nu}^L) \approx 0.87)$ (lower).

incompatibility of the most commonly used mixing rules, the vdW1f, with the structure of mixtures involving volatile solutes as discussed by Chialvo (1993a).

Molecular asymmetry effects on the solvation behavior of the activated complex

It is very difficult to ascribe *a priori* some molecular asymmetry to the activated complex (Kiran and Brennecke, 1993), this being the most troublesome feature of the TST approach. It is also clear that the activated complex is not the product of reaction, and therefore, it may be inappropriate to assign it the product's asymmetry, as is sometimes assumed (Clifford, 1994; Knutson et al., 1995). In light of these difficulties, it appears more insightful to determine how the molecular asymmetry of the activated complex, and consequently its solvation behavior, can affect the kinetic rate constant at near-critical conditions rather than trying to speculate on its molecular description.

For example, by recalling that the isothermal compressibility is a positive definite quantity, we can conclude that the sign of the pressure derivative on the lefthand side of Eq. 5 is determined by the linear combination of the short-range contributions to the species partial molar volumes $\bar{v}_u^\infty(SR)$ such that,

$$\nu_{\Re}\bar{v}_{\Re}^\infty(SR) > \nu_R\bar{v}_R^\infty(SR) + \nu_S\bar{v}_S^\infty(SR) + \Delta\nu\bar{v}_u^{\infty(IG)}(SR) \quad (6)$$

will give rise to $(\partial \ln k^{TST}/\partial P)_{T,x} < 0$, where $\bar{v}_u^{\infty(IG)}(SR)$ is a positive quantity defined by Eq. A16, and $\Delta\nu = \nu_R + \nu_S - \nu_{\Re}$ is typically positive or zero (see Appendix A). Equation 6 clearly indicates that the pressure effect on the rate constant depends on a solvation balance between reactants and activated complex species, that is, on the relative molecular asymmetries of *all* species in solution.

For the sake of simplicity (and to make contact with the previous section) let us first assume that the transition state complex $\Re^\ddagger$ behaves as the reactant R, that is, their molecular asymmetries are identical to each other *regardless of its type*. Thus, a negative pressure effect on the rate constant, $(\partial \ln k^{TST}/\partial P)_{T,x} < 0$, is always possible as long as $\bar{v}_S^\infty(SR) < -(\Delta\nu/\nu_S)\bar{v}_u^{\infty(IG)}(SR) < 0$, that is, when the reactive cosolvent behaves as an "attractive" (Debenedetti and Mohamed, 1989) or nonvolatile species ($(\partial P/\partial x_s)_{T,\rho,x_{k\neq s}}^\infty < 0$ (Levelt Sengers, 1991a)), regardless of the type of solvation behavior of the other species. A similar situation occurs when $\Re^\ddagger$ and S show the same solvation behavior, for example, in that $(\partial \ln k^{TST}/\partial P)_{T,x} < 0$ requires that $\bar{v}_R^\infty(SR) < 0$.

Otherwise, $(\partial \ln k^{TST}/\partial P)_{T,x} > 0$ will be observed at near-critical conditions as long as,

$$\nu_{\Re}\bar{v}_{\Re}^\infty(SR) < \nu_R\bar{v}_R^\infty(SR) + \nu_S\bar{v}_S^\infty(SR) + \Delta\nu\bar{v}_u^{\infty(IG)}(SR). \quad (7)$$

If the transition state complex $\Re^\ddagger$ behaves similarly to the reactant R (or S) species, then the condition of Eq. 7, $\bar{v}_S^\infty(SR) > -(\Delta\nu/\nu_S)\bar{v}_u^{\infty(IG)}(SR)$ (or $\bar{v}_R^\infty(SR) > -(\Delta\nu/\nu_R)\bar{v}_u^{\infty(IG)}(SR)$), is satisfied by a species S (or R) behaving as a repulsive $(0 \lesssim \bar{v}_S^\infty(SR) \leq \rho^{-1})$ solute. Alternatively, note that when $\nu_{\Re}\bar{v}_{\Re}^\infty(SR) \approx \nu_R\bar{v}_R^\infty(SR) + \nu_S\bar{v}_S^\infty(SR) + \Delta\nu\bar{v}_u^{\infty(IG)}(SR)$ in the compressible region of the solvent, $(\partial \ln k^{TST}/\partial P)_{T,x}$ will show a very flat dependence with density (pressure), a behavior already observed by Knutson et al. (1995) for Diels–Alder reactions in propane.

The dependence of the sign of the $(\partial \ln k^{TST}/\partial P)_{T,x}$ on the relative asymmetries between solute species and the solvent becomes more evident when considering the sensitivity of the solvation properties to the solute–solvent combining rules. More precisely, we have used the Lorentz and Berthelot rules throughout our calculations, that is,

$$\epsilon_{u\nu}^B = (\epsilon_{\nu\nu}\epsilon_{uu})^{0.5} \quad (8)$$

$$\sigma_{u\nu}^L = 0.5(\sigma_{\nu\nu} + \sigma_{uu}), \quad (9)$$

where $\nu\nu$ and uu denote solvent-solvent and solute-solute interactions. Note, however, that small perturbations of these rules have profound effects on the corresponding excess properties (Chialvo, 1991). For example, a deviation of 4% on the Berthelot rule, $\xi = (\epsilon_{u\nu}/\epsilon_{u\nu}^B) \approx 0.96$, and 7% on the Lorentz rule, $\eta = (\sigma_{u\nu}/\sigma_{u\nu}^L) \approx 0.93$, for the TS–CO$_2$ interactions, suffices to match the asymmetry of the ^{3}BP–CO$_2$ interactions, and therefore, to change the sign of the pressure dependence in the reaction ^{3}BP + ^{3}O$_2$ + CO$_2$ $\Leftrightarrow$ TS from $(\partial \ln k^{TST}/\partial P)_{T,x} > 0$ to $(\partial \ln k^{TST}/\partial P)_{T,x} < 0$ (Figure 9). Likewise, deviations of $\xi = (\epsilon_{u\nu}/\epsilon_{u\nu}^B) \approx 0.89$ and $\eta = (\sigma_{u\nu}/\sigma_{u\nu}^L) \approx 0.87$ for the TS–CO$_2$ in the ^{3}BP + 1,4-C$_6$ + CO$_2$ $\Leftrightarrow$ TS, will reverse the sign of $(\partial \ln k^{TST}/\partial P)_{T,x}$ from positive to negative (Figure 10).

Isothermal pressure vs. density coefficients of the kinetic rate constant

Because we adjust the system density by manipulating the system pressure, it appears natural to analyze how the system properties change with pressure (as done in the previous section). While there is nothing inherently wrong with this approach, the large and implicit compressibility effects can obscure our interpretation of the actual solvation mechanism. This appears to be the case in the study of the pressure effect on the kinetic rate constant in the vicinity of the solvent critical point, where the solvent becomes highly compressible, that is, where small pressure perturbations induce large changes in density. If we analyze (or measure) the change in the rate constant as a function of the system pressure along a near-critical isotherm, we will inevitably find a large change (increase or decrease) of the rate constant in the vicinity of the solvent critical conditions (unless we have the unlikely situation of zero volume of activation).

Solvation phenomena, by their very nature, involve interactions occurring within nearest coordination shells, that is, finite correlation distances. Near criticality, however, is simply a useful state since it allows adjusting the solvent's solvation power (large changes in density) by small perturbations of the system pressure and temperature. To observe the actual solvent effect we must eliminate the compressibility contribution from Eq. 5 and determine the corresponding density coefficient, that is,

$$\left(\frac{\partial \ln k^{TST}}{\partial \rho}\right)_{T,x} = [\nu_R(\bar{\nu}_R^{\infty}(SR) - \bar{\nu}_R^{\infty(IG)}(SR)) + \nu_S(\bar{\nu}_S^{\infty}(SR) - \bar{\nu}_S^{\infty(IG)}(SR)) - \nu_{\Re}(\bar{\nu}_{\Re}^{\infty}(SR) - \bar{\nu}_{\Re}^{\infty(IG)}(SR))], \quad (10)$$

which not surprisingly indicates that the solvation effects are finite everywhere. At the solvent's critical point, this density derivative becomes proportional to a linear combination of the Krichevskii's parameter of species in solution, that is,

$$\left(\frac{\partial \ln k^{TST}}{\partial \rho}\right)_{T,x}^{c} = \frac{\left[\nu_R(\partial P/\partial x_R)_{\rho_c T_c}^{\infty} + \nu_S(\partial P/\partial x_S)_{\rho_c T_c}^{\infty} - \nu_{\Re}(\partial P/\partial x_{\Re})_{\rho_c T_c}^{\infty}\right]}{kT_c\,\rho_c^2} - \frac{\Delta\nu}{\rho_c}. \quad (11)$$

Therefore, should any "near-critical effects on the kinetic rate constant" exist, Eq. 11 will show it as a change in the behavior of $(\partial \ln k^{TST}/\partial \rho)_{T,x}$ in the vicinity of the solvent's critical point. According to Figures 9 and 10, the righthand side of Eq. 10 exhibits an isothermal quasi-linear dependence with the solvent density, especially in the vicinity of the solvent's critical density. Equations 10–11 support earlier arguments on the advantages of isochoric rather than isobaric studies of the variation of ln k (Eckert, 1972).

Isobaric vs. isochoric temperature coefficients of the kinetic rate constant

An alternative way to tune the solvation power of a near-critical solvent is by manipulation of the system temperature at constant pressure. As done previously, we can factor the temperature coefficient into compressibility and solvation effects as indicated in Appendix B. The resulting expression is

$$\left(\frac{\partial \ln k^{TST}}{\partial T}\right)_{P,x} = \frac{\Delta H_0 + kT - \Delta\nu(\bar{h}_\nu^{ro} - (T/\rho)(\partial P/\partial T)_\rho)}{kT^2} + \int_0^{\rho(P)}\left(\frac{\partial(\nu_R\bar{\nu}_R^{\infty}(SR) + \nu_S\bar{\nu}_S^{\infty}(SR) - \nu_{\Re}\bar{\nu}_{\Re}^{\infty}(SR))}{\partial T}\right)_\rho d\rho - \kappa\rho\left(\frac{\partial P}{\partial T}\right)_\rho [\nu_R(\bar{\nu}_R^{\infty}(SR) - \bar{\nu}_R^{\infty(IG)}(SR)) - \nu_S(\bar{\nu}_S^{\infty}(SR) - \bar{\nu}_S^{\infty(IG)}(SR)) - \nu_{\Re}(\bar{\nu}_{\Re}^{\infty}(SR) - \bar{\nu}_{\Re}^{\infty(IG)}(SR))], \quad (12)$$

where ΔH_0 is the standard heat of formation of the activated complex at the system temperature, $\bar{h}_\nu^{or} = h_\nu^{or}(T,P)$ is the residual molar enthalpy of the pure solvent, and the superscripts IG indicate ideal gas properties. Consequently, the solvation effect becomes

$$\left(\frac{\partial \ln k^{TST}}{\partial T}\right)_{\rho,x} = \frac{\Delta H_0 + kT - \Delta\nu(\bar{h}_\nu^{ro} - (T/\rho)(\partial P/\partial T)_\rho)}{kT^2} + \int_0^{\rho(P)}\left(\frac{\partial(\nu_R\bar{\nu}_R^{\infty}(SR) + \nu_S\bar{\nu}_S^{\infty}(SR) - \nu_{\Re}\bar{\nu}_{\Re}^{\infty}(SR))}{\partial T}\right)_\rho d\rho \quad (13)$$

Summary and Concluding Remarks

In this article we attempt to interpret experimental findings by pointing out that the thermodynamic pressure or temperature coefficient and the species solvation behavior are the macroscopic and microscopic expressions of the same phenomenon, by presenting a statistical mechanical solvation analysis of the thermodynamic pressure or temperature dependence of the kinetics rate constant at near and supercritical conditions.

The solvation formalism tells us that no matter how we approach the system, either microscopically or macroscopically, the macroscopic pressure or temperature coefficient of the kinetic rate constant will reflect the behavior resulting from the actual (local) distributions of reactant and TS species in solution at a microscopic level. Within the framework of the TST, this analysis suggests two immediate consequences: (1) we cannot separate the solvation behavior from the pressure or temperature coefficient in the kinetic analysis, and (2) we cannot assess properly the solvation contribution to the pressure or temperature coefficient by using macroscopic correlations, such as equations of state, due to lack of precise information about the molecular asymmetry of the transition state complex (Brennecke, 1993), its ambiguous connection to the EOS's adjustable parameters, and the consequent inherent inaccuracy of the species partial molar properties (Eckert et al., 1983). An obvious corollary is that the combination of microscopic tools and macroscopic EOS's may lead to ambiguous conclusions about the disagreement between experimental results and EOS predictions.

Thus, before we attempt to seek a plausible explanation for the observed disagreement between experimentally observed and predicted pressure and temperature effects, we must assess the impact of missing information in current kinetic treatments. One aspect usually overlooked when dealing with reactions at high temperature and pressure is the fact that the TST approach could be inaccurate or even invalid for specific reactions in supercritical solvents, and consequently, any attempt to rationalize experimental data based solely on EOS predictions would certainly be meaningless. TST relies on the hypothesis (among others) that the concentration of reactant and TS species are in equilibrium and no barrier recrossing by any species is possible (Hynes, 1985; Reichardt, 1979; Steinfeld et al., 1989). However, the recrossing assumption might become hardly acceptable at near-critical conditions, as a result of the solvent's large density fluctuations, and its validity should be carefully analyzed.

As a sample of this phenomenon, let us consider the kinetics of interconversion of ion-pair configurations in infinitely dilute NaCl aqueous solutions. On the one hand, the simulation results for the transmission coefficient $\chi = k/k^{TST}$ for this reaction at ambient conditions indicate a value of ~ 0.2 (Guàrdia et al., 1991; Rey and Guàrdia, 1992; Smith and Haymet, 1992). On the other hand, our molecular simulation studies at supercritical conditions indicate that this coefficient becomes very small, ~ 0.05 (Chialvo et al., 1997). As a matter of fact, the literature reports transmission coefficients in the range of 1 to 10^{-5} (Hirschfelder et al., 1954), that is, a hardly acceptable approximation for $\chi = 1$.

The alternative treatment of experimental pressure or temperature effect on the kinetic rate constant is to consider explicitly the temperature or pressure dependence of the corresponding transmission coefficients (Van Eldik et al., 1989):

$$k_{\text{exptl}} = \chi(T,P)k^{TST}, \tag{14}$$

so that,

$$\Delta v_{\text{act}}^{\text{exptl}} = \Delta v_{\text{act}}^{TST} - kT\left(\frac{\partial \ln \chi}{\partial P}\right)_{T,x} \tag{15}$$

and

$$\Delta h_{\text{act}}^{\text{exptl}} = \Delta h_{\text{act}}^{TST} + kT^2\left(\frac{\partial \ln \chi}{\partial T}\right)_{P,x}. \tag{16}$$

Thus, activation volumes and energies obtained in the regression of experimental data become effective (apparent) values, in that they include other less obvious effects, and are useful expressions for interpolation purposes. However, and as already emphasized by Whalley (1967), and Troe (1978), these activation quantities cannot be considered within the TST framework unless we first analyze the consequences of the breakdown of the TST.

Acknowledgments

This work was supported by the Division of Chemical Sciences, Office of Basic Energy Sciences, U.S. Department of Energy. Yu. V. Kalyuzhnyi would like to acknowledge the support of the joint INTAS-Ukraine Call'95 grant (INTAS-UA95-133).

Literature Cited

Barker, J. A., and D. Henderson, "What is 'Liquid'? Understanding the States of Matter," *Rev. Mod. Phys.*, **48**, 587 (1976).

Bell, R. P., "The Role of the Solvent in Reaction Kinetics," *Annu. Rep. Prog. Chem.*, **36**, 82 (1939).

Ben-Naim, A., "Theory of Preferential Solvation of Non-Electrolytes," *Cell Biophys.*, **12**, 3694 (1988).

Ben-Naim, A., "Inversion of the Kirkwood-Buff Theory of Solutions and Its Applications," *Fluctuation Theory of Mixtures*, E. Matteoli and G. A. Mansoori, eds., Taylor & Francis, New York, p. 211 (1990).

Benson, S. W., *The Foundation of Chemical Kinetics*, McGraw-Hill, New York (1960).

Benson, S. W., and D. M. Golden, "Methods for the Estimation of Rate Parameters of Elementary Processes," *Physical Chemistry. An Advanced Treatise*, H. Eyring, ed., Academic Press, New York, p. 57 (1975).

Brennecke, J. F., "Spectroscopic Investigation of Reactions in Supercritical Fluids. A Review," *Supercritical Engineering Science. Fundamentals Studies and Applications*, E. Kiran and J. F. Brennecke, eds., American Chemical Society, Washington, DC, p. 201 (1993).

Bruno, T. J., and J. F. Ely, eds., *Supercritical Fluid Technology*, CRC Press, Boca Raton, FL (1991).

Bunker, C. E., and Y.-P. Sun, "Evidence for Enhanced Bimolecular Reactions in Supercritical CO_2 at Near-Critical Densities from a Time-Resolved Study of Fluorescence Quenching of 9,10-Bis(phenylethynyl)anthracene by Carbon Tetrabromine," *J. Amer. Chem. Soc.*, **117**, 10865 (1995).

Carlier, C., and T. W. Randolph, "Dense-Gas Solvent-Solute Clusters at Near-Infinite Dilution: EPR Spectroscopic Evidence," *AIChE J.*, **39**, 876 (1993).

Chateauneuf, J. E., C. B. Roberts, and J. F. Brennecke, "Laser Flash Photolysis Studies of Benzophenone in Supercritical CO_2," *Supercritical Fluid Technology. Theoretical and Applied Approaches in Analytical Chemistry*, F. V. Bright and M. E. P. McNally, eds., American Chemical Society, Washington, DC, p. 106 (1992).

Chialvo, A. A., "Excess Properties of Liquid Mixtures from Computer Simulation: A Coupling-Parameter Approach to the Determination of Their Dependence on Molecular Asymmetry," *Mol. Phys.*, **73**, 127 (1991).

Chialvo, A. A., "Solute-Solute and Solute-Solvent Correlations in Dilute Near-Critical Ternary Mixtures: Mixed Solute and Entrainer Effects," *J. Phys. Chem.*, **97**, 2740 (1993).

Chialvo, A. A., and P. T. Cummings, "Solute-Induced Effects on the Structure and the Thermodynamics of Infinitely Dilute Mixtures," *AIChE J.*, **40**, 1558 (1994).

Chialvo, A. A., and P. T. Cummings, "Comments on 'Near Critical Phase Behavior of Dilute Mixtures,'" *Mol. Phys.*, **84**, 41 (1995).

Chialvo, A. A., P. T. Cummings, J. M. Simonson, and R. E. Mesmer, "Molecular Simulation Study of Speciation in Supercritical Aqueous NaCl Solutions," *J. Mol. Liquids*, **73/74**, 361 (1997).

Chialvo, A. A., Y. V. Kalyuzhnyi, and P. T. Cummings, "Solvation Thermodynamics of Gas Solubility at Sub- and Near Critical Conditions," *AIChE J.*, **42**, 571 (1996).

Clifford, A. A., "Reactions in Supercritical Fluids," *Supercritical Fluids: Fundamentals for Application*, E. Kiran and J. M. H. Levelt Sengers, eds., NATO ASI Ser., Kluwer, Dordrecht, The Netherlands, p. 449–497 (1994).

Combes, J. R., K. P. Johnston, K. E. O'Shea, and M. A. Fox, "Influence of Solvent-Solute and Solute-Solute Clustering on Chemical Reactions in Supercritical Fluids," *Recent Advances in Supercritical Fluid Technology. Theoretical and Applied Approaches to Analytical Chemistry*, F. V. Bright and M. E. P. McNally, eds., ACS Symp. Ser., American Chemical Society, Washington, DC, p. 31 (1992).

Covington, A. K., and K. E. Newman, "Thermodynamics of Preferential Solvation of Electrolytes in Binary Solvent Mixtures," *Adv. Chem. Ser.*, **155**, 153 (1976).

Debenedetti, P. G., and R. S. Mohamed, "Attractive, Weakly Attractive and Repulsive Near-Critical Systems," *J. Chem. Phys.*, **90**, 4528 (1989).

Eckert, C. A., "High Pressure Kinetics in Solution," *Annu. Rev. Phys. Chem.*, **23**, 239 (1972).

Eckert, C. A., and B. L. Knutson, "Molecular Charisma in Supercritical Fluids," *Fluid Phase Equil.*, **83**, 93 (1993).

Eckert, C. A., D. H. Ziger, K. P. Johnston, and T. K. Ellison, "The Use of Partial Molal Volume Data to Evaluate Equations of State for Supercritical Fluid Mixtures," *Fluid Phase Equil.*, **14**, 167 (1983).

Ellington, J. B., and J. F. Brennecke, "Pressure Effect on the Esterification of Phthalic Anhydride in Supercritical CO_2," *J. Chem. Soc. Chem. Commun.*, **13**, 1094 (1993).

Ellington, J. B., K. M. Park, and J. F. Brennecke, "The Effect of Local Composition Enhancement on the Esterification of Phthalic Anhydride with Methanol in Supercritical Carbon Dioxide," *Ind. Eng. Chem. Res.*, **33**, 965 (1994).

Frost, A. A., and R. F. Pearson, *Kinetics and Mechanism*, Wiley, New York (1961).

Guàrdia, E., R. Rey, and J. A. Padró, "Na^+-Na^+ and Cl^--Cl^- Ion Pairs in Water: Mean Force Potentials by Constrained Molecular Dynamics," *J. Chem. Phys.*, **95**, 2823 (1991).

Hansen, J. P., and I. R. McDonald, *Theory of Simple Liquids*, Academic Press, New York (1986).

Hirschfelder, J. O., C. F. Curtiss, and R. B. Bird, *Molecular Theory of Gases and Liquids*, Wiley, New York (1954).

Hutchenson, K. W., and N. R. Foster, *Innovations in Supercritical Fluids: Science and Technology*, American Chemical Society, Washington, DC (1995).

Hynes, J. T., "The Theory of Reactions in Solution," *Theory of Chemical Reaction Dynamics*, M. Baer, ed., CRC Press, Boca Raton, FL, p. 171 (1985).

Kiran, E., and J. F. Brennecke, eds., *Supercritical Engineering Science. Fundamentals Studies and Applications*, ACS Symp. Ser., American Chemical Society, Washington, DC (1993).

Kiran, E., and J. M. H. Levelt Sengers, *Supercritical Fluids. Fundamentals for Applications*, Kluwer, Dordrecht, The Netherlands (1994).

Kirkwood, J. G., and F. P. Buff, "The Statistical Mechanical Theory of Solution. I," *J. Chem. Phys.*, **19**, 774 (1951).

Knutson, B. L., A. K. Dillow, C. L. Liotta, and C. A. Eckert, "Kinetics of a Diels-Alder Reaction in Supercritical Propane," *Innovations in Supercritical Fluids: Science and Technology*, K. W. Hutchenson and N. R. Foster, eds., American Chemical Society, Washington, DC, p. 166 (1995).

Levelt Sengers, J. M. H., "Thermodynamics of Solutions Near the Solvent's Critical Point," *Supercritical Fluid Technology*, T. J. Bruno and J. F. Ely, eds., CRC Press, Boca Raton, FL, p. 1 (1991a).

Levelt Sengers, J. M. H., "Solubility Near the Solvent's Critical Point," *J. Supercrit. Fluids*, **4**, 215 (1991b).

Martin, H., "Kinetic Relationships Between Reactions in the Gas Phase and in Solution," *Angew. Chem. (I.E.)*, **5**, 78 (1966).

McDonald, I. R., "Equilibrium Theory of Liquid Mixtures," *Statistical Mechanics*, K. Singer, ed., The Chemical Society, London, p. 134 (1973).

McHugh, M. A., and V. J. Krukonis, *Supercritical Fluid Extraction: Principles and Practice*, Butterworths, Boston (1994).

Milner, S. T., and P. C. Martin, "Critical Slowing of Chemical Reactions," *Phys. Rev. A*, **33**, 1996 (1986).

Moelwyn-Hughes, E. A., *The Chemical Statics and Kinetics of Solutions*, Academic Press, London (1971).

O'Connell, J. P., "Thermodynamic Properties of Solutions Based on Correlation Functions," *Mol. Phys.*, **20**, 27 (1971).

Panagiotopoulos, A. Z., "Direct Determination of Phase Coexistence Properties of Fluids by Monte Carlo Simulation in a New Ensemble," *Mol. Phys.*, **61**, 813 (1987).

Prausnitz, J. M., R. N. Lichtenthaler, and E. G. de Azevedo, *Molecular Thermodynamics of Fluid Phase Equilibria*, Prentice Hall, Englewood Cliffs, NJ (1986).

Reichardt, C., *Solvent Effects in Organic Chemistry*, Verlag Chemie, Weinheim, Germany (1979).

Rey, R., and E. Guàrdia, "Dynamical Aspects of the Na+Cl− Ion Pair Association in Water," *J. Phys. Chem.*, **96**, 4712 (1992).

Roberts, C. B., J. F. Brennecke, and J. E. Chateauneuf, "Solvation Effects on Reactions of Triplet Benzophenone in Supercritical Fluids," *AIChE J.*, **41**, 1306 (1995a).

Roberts, C. B., J. Zhang, J. E. Chateauneuf, and J. F. Brennecke, "Laser Flash Photolysis and Integral Equation Theory to Investigate Reactions of Dilute Solutes with Oxygen in Supercritical Fluids," *J. Amer. Chem. Soc.*, **117**, 6553 (1995b).

Savage, P. E., S. Golapan, T. I. Mizan, C. J. Martino, and E. E. Brock, "Reactions at Supercritical Conditions: Applications and Fundamentals," *AIChE J.*, **41**, 1723 (1995).

Smith, D. E., and A. D. J. Haymet, "Structure and Dynamics of Water and Aqueous Solutions: The Role of Flexibility," *J. Chem. Phys.*, **96**, 8450 (1992).

Steinfeld, J. I., J. S. Francisco, and W. L. Hase, *Chemical Kinetics and Dynamics*, Prentice Hall, Englewood Cliffs, NJ (1989).

Sun, Y.-P., and C. E. Bunker, "Quantitative Spectroscopic Investigation of Enhanced Excited State Complex Formation in Supercritical Carbon Dioxide Under Near-Critical Conditions: Inconsistency Between Experimental Evidence and Classical Photophysical Mechanism," *J. Phys. Chem.*, **99**, 13778 (1995).

Troe, J., "Kinetic Phenomena in Gases at High Pressure," *High Pressure Chemistry*, H. Kelm, ed., NATO ASI Ser., Reidel, Dordrecht, The Netherlands, p. 489 (1978).

Van Eldik, R., T. Asano, and W. J. Le Noble, "Activation and Reaction Volumes in Solutions: 2," *Chem. Rev.*, **89**, 549 (1989).

Whalley, E., "High Pressure," *Ann. Rev. Phys. Chem.*, **18**, 205 (1967).

Wheeler, J. C., and R. G. Petschek, "Anomalies in Chemical Equilibria Near Critical Points of Dilute Solutions," *Phys. Rev. A*, **28**, 2442 (1983).

Zhang, J., L. L. Lee, and J. F. Brennecke, "Fluorescence Spectroscopy and Integrals Equation Studies of Preferential Solvation in Supercritical Fluid Mixtures," *J. Phys. Chem.*, **99**, 9268 (1995).

Appendix A: Derivation of Eq. 4

To make contact with the corresponding change of free energies we rewrite $K_c^\ddagger$ in terms of the thermodynamic equilibrium constant, that is, in terms of the species fugacities (Prausnitz et al., 1986)

$$K_f^\ddagger(T) = \frac{\left(Px_{\Re}\hat{\phi}_{\Re}\right)^{\nu_{\Re}}}{\left(Px_R\hat{\phi}_R\right)^{\nu_R}\left(Px_S\hat{\phi}_S\right)^{\nu_S}}, \qquad \text{(A1)}$$

which, after replacing the mole fractions by the corresponding ratios of number densities, we obtain,

$$K_c^\ddagger = K_f^\ddagger(T)P^{\Delta\nu}\rho^{-\Delta\nu}\frac{\hat{\phi}_R^{\nu_R}\hat{\phi}_S^{\nu_S}}{\hat{\phi}_{\Re}^{\nu_{\Re}}}, \qquad \text{(A2)}$$

where $\Delta\nu = \nu_R + \nu_S - \nu_{\Re}$. Now, from Eqs. 2, A1, and A2 the reaction rate constant reads,

$$k^{TST} = \frac{kTK_0}{\hbar}K_f^\ddagger(T)P^{\Delta\nu}\rho^{-\Delta\nu}\frac{\hat{\phi}_R^{\nu_R}\hat{\phi}_S^{\nu_S}}{\hat{\phi}_{\Re}^{\nu_{\Re}}}, \qquad \text{(A3)}$$

so that its pressure derivative, at constant temperature and composition, becomes

$$\left(\frac{\partial \ln k^{TST}}{\partial P}\right)_{T,x} = \frac{\Delta\nu}{P} - \Delta\nu\left(\frac{\partial \ln \rho}{\partial P}\right)_{T,x} + \nu_R\left(\frac{\partial \ln \hat{\phi}_R}{\partial P}\right)_{T,x} + \nu_S\left(\frac{\partial \ln \hat{\phi}_S}{\partial P}\right)_{T,x} - \nu_{\Re}\left(\frac{\partial \ln \hat{\phi}_{\Re}}{\partial P}\right)_{T,x}. \qquad \text{(A4)}$$

Here we are interested in highly dilute reactants, therefore, Eq. A4 is taken at infinite dilution, that is,

$$\left(\frac{\partial \ln k^{TST}}{\partial P}\right)_{T,x} = \frac{\Delta \nu}{P} - \Delta \nu \left(\frac{\partial \ln \rho}{\partial P}\right)_{T,x} + \nu_R \left(\frac{\partial \ln \hat{\phi}_R^{\infty}}{\partial P}\right)_{T,x}$$
$$+ \nu_S \left(\frac{\partial \ln \hat{\phi}_S^{\infty}}{\partial P}\right)_{T,x} - \nu_{\Re} \left(\frac{\partial \ln \hat{\phi}_{\Re}^{\infty}}{\partial P}\right)_{T,x}$$
$$= -\Delta \nu \kappa + (\nu_R \bar{\nu}_R^{\infty} + \nu_S \bar{\nu}_S^{\infty} - \nu_{\Re} \bar{\nu}_{\Re}^{\infty})/kT, \quad \text{(A5)}$$

where κ is the isothermal compressibility of the pure solvent, $\bar{\nu}_u$ indicates the partial molar volume of species u, and the superscript ∞ denotes infinite dilution. Now, after invoking the following identity (Chialvo and Cummings, 1995),

$$\bar{\nu}_u^{\infty} = \rho^{-1}\left[1 + \kappa \left(\frac{\partial P}{\partial x_u}\right)^{\infty}_{T,\rho,x_{k\neq u}}\right] \quad \text{(A6)}$$

Equation A5 becomes

$$\left(\frac{\partial \ln k^{TST}}{\partial P}\right)_{T,x} = -\Delta \nu \kappa + \Delta \nu (\rho k T)^{-1}$$
$$+ \kappa \Big[\nu_R (\partial P/\partial x_R)^{\infty}_{T,\rho,x_{k\neq R}} + \nu_S (\partial P/\partial x_S)^{\infty}_{T,\rho,x_{k\neq S}}$$
$$- \nu_{\Re} (\partial P/\partial x_{\Re})^{\infty}_{T,\rho,x_{k\neq \Re}}\Big], \quad \text{(A7)}$$

where we identify (Chialvo and Cummings, 1994)

$$\left(\frac{\partial P}{\partial x_u}\right)^{u}_{\rho\ T,x_{k\neq u}} = \rho^2 kT(\bar{\nu}_u^{\infty}(SR) - \bar{\nu}_\nu^0) \quad \text{(A8)}$$

in terms of the short-range contributions to the partial molar volume of species u at infinite dilution in the solvent. Thus,

$$\left(\frac{\partial \ln k^{TST}}{\partial P}\right)_{T,x} = \Delta \nu (\kappa^{IG} - \kappa) + \kappa \rho [\nu_R (\bar{\nu}_R^{\infty}(SR) - \bar{\nu}_\nu^o)$$
$$+ \nu_S (\bar{\nu}_S^{\infty}(SR) - \bar{\nu}_\nu^o) - \nu_{\Re} (\bar{\nu}_{\Re}^{\infty}(SR) - \bar{\nu}_\nu^o)], \quad \text{(A9)}$$

which highlights the effect of the species solvation contributions $(\bar{\nu}_u^{\infty}(SR) - \bar{\nu}_\nu^o)$.

To make contact with the microstructure of the system we express $(\partial P/\partial x_u)^{\infty}_{T,\rho,x_{k\neq u}}$ in terms of total pair correlation function integrals (TPCFI), or alternatively, in terms of direct pair correlation function integrals (DPCFI) as follows (Chialvo and Cummings, 1994; Chialvo et al., 1996),

$$\left(\frac{\partial P}{\partial x_u}\right)^{\infty}_{\rho,T,x_{k\neq u}} = \rho kT(C^o_{\nu\nu} - C^{\infty}_{u\nu})$$
$$= \frac{\rho^2 kT(G^o_{\nu\nu} - G^{\infty}_{u\nu})}{1 + \rho G^o_{\nu\nu}}, \quad \text{(A10)}$$

so that, the short-range portion of the species partial molar volume at infinite dilution becomes

$$\bar{\nu}_u^{\infty}(SR) = \bar{\nu}_\nu^o + (\kappa^{IG}/\kappa)(G^o_{\nu\nu} - G^o_{u\nu})$$
$$= \bar{\nu}_\nu^o(1 + C^o_{\nu\nu} - C^{\infty}_{u\nu}), \quad \text{(A11)}$$

where $\bar{\nu}_\nu^o = \rho^{-1}$, subscript ν denotes solvent, and the correlation function integrals are given by (O'Connell, 1971)

$$C_{\alpha\beta} = 4\pi\rho \int_0^{\infty} c_{\alpha\beta}(r) r^2\, dr \quad \text{(A12)}$$

and (Kirkwood and Buff, 1951)

$$G_{\alpha\beta} = 4\pi \int_0^{\infty} (g_{\alpha\beta}(r) - 1) r^2\, dr, \quad \text{(A13)}$$

where $c_{\alpha\beta}(r)$ and $g_{\alpha\beta}(r)$ are the direct and total pair correlation functions, respectively (Hansen and McDonald, 1986).

There are three important references for the behavior of $(\partial P/\partial x_u)^{\infty}_{T,\rho,x_{k\neq u}}$ and its associate $\bar{\nu}_u^{\infty}(SR)$, namely: (a) an ideal solution; (b) an ideal gas solute in a real fluid; and (c) an ideal gas solute in an ideal gas solvent. The first case is trivial since $\bar{\nu}_u^{\infty}(IS) = \bar{\nu}_\nu^o = \rho^{-1}$, and therefore $(\partial P/\partial x_u)^{\infty}_{T,\rho,x_{k\nu u}} = 0$. For the two other cases, the virial theorem allows us to show that for an ideal gas solute in a real solvent (Hansen and McDonald, 1986),

$$\left(\frac{\partial P}{\partial x_u}\right)^{\infty}_{\rho,T,x_{k\neq u}} = \rho kT - \kappa^{-1}, \quad \text{(A14)}$$

and consequently that

$$\bar{\nu}_u^{\infty(IG)} = kT\kappa \quad \text{(A15)}$$

$$\bar{\nu}_u^{\infty(IG)}(SR) = \bar{\nu}_\nu^o(2 - (\kappa^{IG}/\kappa)). \quad \text{(A16)}$$

Now, if the solvent becomes an ideal gas, that is, $\kappa \rightarrow \kappa^{IG}$ and $\rho \rightarrow (P/kT)$, then Eqs. A14–A16 reduce to

$$\left(\frac{\partial P}{\partial x_u}\right)^{\infty}_{\rho,T,x_{k\neq u}} = 0 \quad \text{(A17)}$$

and

$$\bar{\nu}_u^{\infty} = \bar{\nu}_u^{\infty}(SR) = P/kT. \quad \text{(A18)}$$

The expressions Eqs. A15–A16 in conjunction with Eq. A9 suggest yet another appealing form for the thermodynamic pressure effect. By recognizing that

$$(\kappa^{IG} - \kappa) = \kappa((\kappa^{IG}/\kappa) - 1)$$
$$= -\kappa\rho(\bar{\nu}_u^{\infty(IG)}(SR) - \bar{\nu}_\nu^o), \quad \text{(A19)}$$

then

$$\Delta \nu (\kappa^{IG} - \kappa) = -\kappa\rho[\nu_R(\bar{\nu}_R^{\infty(IG)}(SR) - \bar{\nu}_\nu^o)$$
$$+ \nu_S(\bar{\nu}_S^{\infty(IG)}(SR) - \bar{\nu}_\nu^o) - \nu_{\Re}(\bar{\nu}_{\Re}^{\infty(IG)}(SR) - \bar{\nu}_\nu^o)], \quad \text{(A20)}$$

so that, by replacing Eq. A20 in Eq. A9, we have

$$\left(\frac{\partial \ln k^{TST}}{\partial P}\right)_{T,x} = \kappa\rho[\nu_R(\bar{\nu}_R^{\infty}(SR) - \bar{\nu}_R^{\infty(IG)}(SR))$$

$$+ \nu_S(\bar{\nu}_S^{\infty}(SR) - \bar{\nu}_S^{\infty(IG)}(SR)) - \nu_{\Re}(\bar{\nu}_{\Re}^{\infty}(SR) - \bar{\nu}_{\Re}^{\infty(IG)}(SR))], \tag{A21}$$

and therefore, that

$$\left(\frac{\partial \ln k^{TST}}{\partial \rho}\right)_{T,x} = [\nu_R(\bar{\nu}_R^{\infty}(SR) - \bar{\nu}_R^{\infty(IG)}(SR))$$

$$+ \nu_S(\bar{\nu}_S^{\infty}(SR) - \bar{\nu}_S^{\infty(IG)}(SR) - \nu_{\Re}(\bar{\nu}_{\Re}^{\infty}(SR) - \bar{\nu}_{\Re}^{\infty(IG)}(SR))] \tag{A22}$$

Appendix B: Derivation of Eq. 12

From Eq. A3 we have that

$$\left(\frac{\partial \ln k^{TST}}{\partial T}\right)_{P,x} = \frac{\Delta H_0}{kT^2} + \frac{1}{T} - \Delta\nu\left(\frac{\partial \ln \rho}{\partial T}\right)_{P,x}$$

$$+ \nu_R\left(\frac{\partial \ln \hat{\phi}_R}{\partial T}\right)_{P,x} + \nu_S\left(\frac{\partial \ln \hat{\phi}_S}{\partial T}\right)_{P,x} - \nu_{\Re}\left(\frac{\partial \ln \hat{\phi}_{\Re}}{\partial T}\right)_{P,x}$$

$$= \Delta h_{\text{act}}/kT^2, \tag{B1}$$

where $\alpha_p = -(\partial \ln \rho/\partial T)_{P,x}$ is the thermal expansivity of the solvent, and ΔH_0 is the standard heat of formation of the activated complex at the temperature of the system. By invoking the following identity

$$(\partial \ln \phi_u^{\infty}/\partial T)_P = \frac{-\bar{h}_u^{r\infty}}{kT^2}, \tag{B2}$$

where $\bar{h}_u^{r\infty}$ is the residual partial molar enthalpy of an infinitely dilute solute u, Eq. B1 becomes

$$\left(\frac{\partial \ln k^{TST}}{\partial T}\right)_{P,x} = \frac{\Delta H_0}{kT^2} + \frac{1}{T} + \Delta\nu\alpha_p$$

$$-(kT^2)^{-1}\left(\nu_R\bar{h}_R^{r\infty} + \nu_S\bar{h}_S^{r\infty} - \nu_{\Re}\bar{h}_{\Re}^{r\infty}\right). \tag{B3}$$

In an earlier work (Chialvo and Cummings, 1994) we showed that $\bar{h}_u^{r\infty}$ is given by

$$\bar{h}_u^{r\infty}(T,P) = -\int_0^{\rho(P)}(\partial C_{u\nu}^{\infty}/\partial\beta)_\rho\frac{d\rho}{\rho} - \beta^{-1} - \beta\left(\frac{\partial P}{\partial\beta}\right)_\rho\bar{\nu}_u^{\infty}, \tag{B4}$$

and the corresponding expression for the residual partial molar enthalpy of the pure solvent by

$$h_\nu^{ro}(T,P) = -\int_0^{\rho(P)}(\partial C_{\nu\nu}^{o}/\partial\beta)_\rho\frac{d\rho}{\rho} - \beta^{-1} - \left(\frac{\beta}{\rho}\right)\left(\frac{\partial P}{\partial\beta}\right)_\rho. \tag{B5}$$

Therefore, from Eqs. B4–B5 we have that

$$\bar{h}_u^{r\infty}(T,P) = \bar{h}_\nu^{ro}(T,P) -$$

$$-\int_0^{\rho(P)}(\partial(C_{u\nu}^{\infty} - C_{\nu\nu}^{o})/\partial\beta)_\rho\frac{d\rho}{\rho} - \left(\frac{\beta}{\rho}\right)\left(\frac{\partial P}{\partial\beta}\right)_\rho(\rho\bar{\nu}_u^{\infty} - 1). \tag{B6}$$

In addition, from Eq. A11 we also have that

$$(\partial(C_{u\nu}^{\infty} - C_{\nu\nu}^{o})/\partial\beta)_\rho = -\rho(\partial\bar{\nu}_u^{\infty}(SR)/\partial\beta)_\rho, \tag{B7}$$

as well as, from Eqs. A6 and A8, that

$$\rho\bar{\nu}_u^{\infty} - 1 = \kappa\left(\frac{\partial P}{\partial x_u}\right)_{T,\rho,x_{k\neq u}}^{\infty}$$

$$= \kappa\rho^2 kT(\bar{\nu}_u^{\infty}(SR) - \rho^{-1}). \tag{B8}$$

Thus, Eq. B6 becomes

$$\bar{h}_u^{r\infty}(T,P) = \bar{h}_\nu^{ro}(T,P)$$

$$+\int_0^{\rho(P)}(\partial\bar{\nu}_u^{\infty}(SR)/\partial\beta)_\rho d\rho - \kappa\left(\frac{\partial P}{\partial\beta}\right)_\rho(\rho\bar{\nu}_u^{\infty}(SR) - 1). \tag{B9}$$

Finally, by introducing Eq. B9 into Eq. B3, and after some rearrangements, we have that

$$\left(\frac{\partial \ln k^{TST}}{\partial T}\right)_{P,x} = \frac{\Delta H_0 - \Delta\nu\bar{h}_\nu^{ro}}{kT^2} + \frac{1}{T} + \Delta\nu\left(\alpha_p + \kappa\left(\frac{\partial P}{\partial T}\right)_\rho\right)$$

$$+\int_0^{\rho(P)}\left(\frac{\partial(\nu_R\bar{\nu}_R^{\infty}(SR) + \nu_S\bar{\nu}_S^{\infty}(SR) - \nu_{\Re}\bar{\nu}_{\Re}^{\infty}(SR))}{\partial T}\right)_\rho d\rho$$

$$-\kappa\rho\left(\frac{\partial P}{\partial T}\right)_\rho(\nu_R\bar{\nu}_R^{\infty}(SR) + \nu_S\bar{\nu}_S^{\infty}(SR) - \nu_{\Re}\bar{\nu}_{\Re}^{\infty}(SR)). \tag{B10}$$

If we recall that $\alpha_p = \kappa(\partial P/\partial T)_\rho$, from Eq. B10 we have,

$$\Delta h_{\text{act}} = \Delta H_0 + kT - \Delta\nu\bar{h}_\nu^{ro}$$

$$+ kT^2\int_0^{\rho(P)}\left(\frac{\partial(\nu_R\bar{\nu}_R^{\infty}(SR) + \nu_S\bar{\nu}_S^{\infty}(SR) - \nu_{\Re}\bar{\nu}_{\Re}^{\infty}(SR))}{\partial T}\right)_\rho d\rho$$

$$-\kappa\rho kT^2\left(\frac{\partial P}{\partial T}\right)_\rho[\nu_R(\bar{\nu}_R^{\infty}(SR) - \rho^{-1}) - \nu_S(\bar{\nu}_S^{\infty}(SR) - \rho^{-1})$$

$$-\nu_{\Re}(\bar{\nu}_{\Re}^{\infty}(SR) - \rho^{-1})] + \Delta\nu kT\left(\frac{\alpha_p}{\alpha_p^{IG}}\right), \tag{B11}$$

where $\alpha_p^{IG} = T^{-1}$. Please compare Eq. B11 with Eq. A14. By recognizing that $kT(\alpha_p/\alpha_p^{IG}) = (T/\rho)(\partial P/\partial T)_\rho$, Eq. B11 becomes

$$\Delta h_{\text{act}} = \Delta H_0 + kT - \Delta\nu(\bar{h}_\nu^{ro} - (T/\rho)(\partial P/\partial T)_\rho)$$
$$+ kT^2 \int_0^{\rho(P)} \left(\frac{\partial(\nu_R \bar{\nu}_R^\infty(SR) + \nu_S \bar{\nu}_S^\infty(SR) - \nu_{\Re} \bar{\nu}_{\Re}^\infty(SR))}{\partial T} \right)_\rho d\rho$$
$$- \kappa \rho k T^2 \left(\frac{\partial P}{\partial T} \right)_\rho [\nu_R(\bar{\nu}_R^\infty(SR) - \bar{\nu}_R^{\infty(IG)}(SR)) - \nu_S(\bar{\nu}_S^\infty(SR)$$
$$- \bar{\nu}_S^{\infty(IG)}(SR)) - \nu_{\Re}(\bar{\nu}_{\Re}^\infty(SR) - \bar{\nu}_{\Re}^{\infty(IG)}(SR))]. \quad \text{(B12)}$$

We might also want to study the temperature derivative at constant density (instead of pressure), that is,

$$\left(\frac{\partial \ln k^{TST}}{\partial T} \right)_{\rho,x} = \left(\frac{\partial \ln k^{TST}}{\partial T} \right)_{P,x} + \left(\frac{\partial P}{\partial T} \right)_{\rho,x} \left(\frac{\partial \ln k^{TST}}{\partial P} \right)_{T,x}, \quad \text{(B13)}$$

so that, by replacing Eqs. A14 and B10 in Eq. B13 we obtain

$$\left(\frac{\partial \ln k^{TST}}{\partial T} \right)_{\rho,x} = \frac{\Delta H_0 + kT - \Delta\nu(\bar{h}_\nu^{ro} - (T/\rho)(\partial P/\partial T)_\rho)}{kT^2}$$
$$+ \int_0^{\rho(P)} \left(\frac{\partial(\nu_R \bar{\nu}_R^\infty(SR) + \nu_S \bar{\nu}_S^\infty(SR) - \nu_{\Re} \bar{\nu}_{\Re}^\infty(SR))}{\partial T} \right)_\rho d\rho, \quad \text{(B14)}$$

which tells us that the density dependence of temperature effect on the kinetic rate constant is always finite, the result of solvation contributions.

Manuscript received July 18, 1997, and revision received Nov. 17, 1997.